JOURNAL OF MAGNETIC RESONANCE **131,** 232–240 (1998)
ARTICLE NO. MN981364

Effective Gradients in Porous Media Due to Susceptibility Differences

Martin D. Hürlimann

Schlumberger-Doll Research, Ridgefield, Connecticut 06877-4108

Received April 7, 1997; revised September 30, 1997

In porous media, magnetic susceptibility differences between the solid phase and the fluid filling the pore space lead to field inhomogeneities inside the pore space. In many cases, diffusion of the spins in the fluid phase through these internal inhomogeneities controls the transverse decay rate of the NMR signal. In disordered porous media such as sedimentary rocks, a detailed evaluation of this process is in practice not possible because the field inhomogeneities depend not only on the susceptibility difference but also on the details of the pore geometry. In this report, the major features of diffusion in internal gradients are analyzed with the concept of effective gradients. Effective gradients are related to the field inhomogeneities over the dephasing length, the typical length over which the spins diffuse before they dephase. For the CPMG sequence, the dependence of relaxation rate on echo spacing can be described to first order by a distribution of effective gradients. It is argued that for a given susceptibility difference, there is a maximum value for these effective gradients, g_{max}, that depends on only the diffusion coefficient, the Larmor frequency, and the susceptibility difference. This analysis is applied to the case of water-saturated sedimentary rocks. From a set of NMR measurements and a compilation of a large number of susceptibility measurements, we conclude that the effective gradients in carbonates are typically smaller than gradients of current NMR well logging tools, whereas in many sandstones, internal gradients can be comparable to or larger than tool gradients.

INTRODUCTION

When a fluid-saturated porous medium is placed in a homogeneous magnetic field for NMR measurements, susceptibility differences between the solid matrix and the pore fluid can lead to substantial magnetic field gradients in the pore space. These susceptibility-induced gradients are called ''internal gradients'' and it is well known that they can affect NMR measurements in various ways. Diffusion of spins in these inhomogeneities leads to extra transverse relaxation. The internal gradients can also interfere with externally applied gradients and cause distortions in imaging or diffusion measurements. These internal gradients depend both on the susceptibility difference between the matrix and fluid and on the pore geometry.

There are several types of porous media where susceptibility-induced field inhomogeneities are relevant. Biological samples can have significant internal gradients, especially at high magnetic fields. Functional MRI (*1, 2*) relies on changes in the internal gradients that are caused by changes in susceptibility. Paramagnetic contrast agents are routinely used in medical MRI to deliberately create internal field inhomogeneities (*3–5*). In this paper, we will concentrate on water-saturated sedimentary rocks. In these systems, paramagnetic impurities in the rock grain lead to a susceptibility difference that can vary by orders of magnitude from rock to rock, depending on the impurity concentration.

Nuclear magnetic resonance measurements on the fluid phase has become a standard technique for studying the pore geometry of sedimentary rocks (*6*). In the most common measurement, the CPMG sequence is used to measure the surface-induced relaxation rate of the transverse magnetization, a measure of the local ratio of surface area to pore volume. The effects of internal gradients are minimized by using low fields and the shortest possible echo spacing, t_E. The dependence of the measured relaxation time on echo spacing and Larmor frequency has been studied by Kleinberg and Horsfield (*7, 8*) and by the group of Brown, Borgia, and Fantazzini (*9, 10*).

The commercial NMR logging tools currently used in well logging (*11, 12*) have tool-related gradients that are of the order of a few tens of gauss per centimeter. Recently, Akkurt *et al.* (*13*) have proposed to take advantage of the tool gradients and to obtain information about the diffusion coefficient of the fluid from the t_E dependence of the measured relaxation time. The general fluid identification by the method of diffusion measurements in the tool gradient is successful only if the total gradient in the pore space is dominated by the tool gradient and not by the internal gradients. In this report, we discuss the size of typical internal gradients in sedimentary rocks.

We first review the basic physics of restricted diffusion in a gradient for the Hahn echo and identify the key parameters governing the NMR decay rate. We then discuss qualitatively the effects on a CPMG sequence. For disordered systems, the local gradient of the magnetic field in the pore space can be very high. It is argued that the relevant quantities for NMR measurements are not the local gradients, but some effective gradients related to the local field inhomogeneities averaged

1090-7807/98 $25.00

over the dephasing length. The dephasing length depends on the diffusion properties. For a given susceptibility difference, these effective internal gradients have an upper bound, which depends simply on the susceptibility difference, the Larmor frequency, and the diffusion coefficient. Laboratory data of susceptibility measurements on 321 rocks are analyzed and a probability distribution of the maximal internal gradient is obtained. In the last part of this report, CPMG measurements with a wide range of echo spacings are analyzed for sedimentary rocks with different susceptibilities. The data are compared with the analysis outlined above.

HAHN ECHO IN A CONSTANT GRADIENT AND SIMPLE GEOMETRY

We first summarize results for the spin echo decay for spins diffusing in a constant gradient and restricted between two parallel plates, separated by a distance l_s. Stoller *et al.* (*14*) and de Swiet and Sen (*15*) have discussed the exact solution and showed that this seemingly simple case is already very difficult to solve exactly. For the purpose of this paper, it is sufficient to describe the main behavior and discuss how it is modified in a more general case.

In simple geometries characterized by a single length scale, l_s, the decay of the Hahn echo in a gradient, g, is governed by the interplay of three lengths (*14, 16*):

1. the diffusion length, $l_D \equiv \sqrt{D_0\tau}$ (D_0 is the molecular self-diffusion coefficient);
2. the size of the pore or structure, l_s; and
3. the dephasing length, $l_g \equiv \{D_0/(\gamma g)\}^{1/3}$ (γ is the gyromagnetic ratio).

The diffusion length gives a measure of the average distance that a spin diffuses during the time τ. For water at room temperature, l_D can be as long as 50 μm. The dephasing length l_g may be thought of as the typical length scale over which a spin must travel to dephase by 2π radians. It depends weakly on gradient strength. For g in the range of 1 to 1000 G/cm and water at room temperature, l_g varies between about 10 and 1 μm.

In the analysis of the spin echo decay, three asymptotic behaviors can be identified. We have called them the free diffusion regime, the motional averaging regime, and the localization regime, respectively (*16*). The shortest of the three length scales, $\{l_D, l_s, \text{or } l_g\}$, determines which of the three asymptotic regimes applies. If the diffusion length l_D is shorter than the other two length scales, the spin echo decay will be predominantly described by the free diffusion regime. If the pore size l_s is shortest, the motional averaging regime applies. And finally, when the dephasing length l_g becomes the shortest length, the localization regime describes the decay asymptotically.

At short enough diffusion times, l_D is always the shortest length. The majority of spins have not experienced the effect of restrictions and the decay is well approximated by the free diffusion regime,

$$M(\tau)/M_0 = \exp\left\{-\frac{2}{3}D_0\gamma^2 g^2\tau^3\right\} = \exp\left\{-\frac{2}{3}\left(\frac{l_D}{l_g}\right)^6\right\}, \quad [1]$$

where M_0 is the signal amplitude at zero gradient strength.

At longer diffusion times when the diffusion length l_D becomes larger than the structural length l_s or the dephasing length l_g, the behavior depends on the ratio l_s/l_g. When this ratio is small compared to 1 (i.e., in small pores where l_s becomes the shortest length), the spins average out the field inhomogeneities. This is the motional averaging regime. Asymptotically, the echo amplitude for $\tau \gg (l_s^2/D_0)$ decays like

$$M(\tau)/M_0 = \exp\left\{-\frac{1}{120}\frac{\gamma^2 g^2 l_s^4 2\tau}{D_0}\right\} = \exp\left\{-\frac{1}{60}\left(\frac{l_D}{l_g}\right)^2\left(\frac{l_s}{l_g}\right)^4\right\}. \quad [2]$$

Equation [2] is appropriate for parallel plates, separated by a distance l_s. In other geometries, Neuman (*17*) showed that the decay has the same form as in Eq. [2], but with a different numerical prefactor in the exponent.

In larger pores, where $l_s/l_g \gg 1$, the decay of the spin echo starts to deviate significantly from Eq. [1] much before the spins have traversed a pore, $\tau_s \approx (l_s^2/D_0)$. When the echo amplitude has decayed to a level that scales likes l_g/l_s, the dephasing length l_g becomes the shortest length and the localization regime is reached (*16*):

$$M(\tau)/M_0 = 5.88\frac{l_g}{l_s}\exp\{-1.02\,\gamma^{2/3}g^{2/3}D_0^{1/3}\tau\} = 5.88\frac{l_g}{l_s}\exp\left\{-1.02\left(\frac{l_D}{l_g}\right)^2\right\}. \quad [3]$$

The exponent, proportional to τ and $g^{2/3}$, is independent of the exact geometry, but the prefactor 5.88 is modified for other geometries (*15*).

To get a qualitative idea of the dependence on the size l_s, the asymptotic expressions of Eqs. [1] to [3] are plotted in Fig. 1. Here it is assumed that the spins are confined between two parallel plates, separated by a distance l_s, and that the gradient is uniform and scales inversely with the plate separation: $g = \Delta\omega/(\gamma l_s)$. The range of Larmor frequencies, $\Delta\omega$, is assumed to be independent of size, as is the case when it is caused by susceptibility differences. It is natural

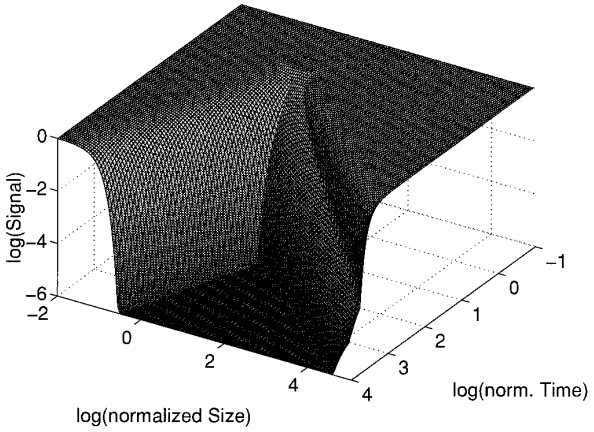

FIG. 1. Asymptotic Hahn spin echo decay for spins diffusing between two parallel plates separated by size l_s and in a constant gradient $g = \Delta\omega/(\gamma l_s)$. The logarithm (base 10) of the signal is plotted as a function of the logarithm of normalized time, $\log_{10}(\Delta\omega t)$, and the logarithm of normalized size, $\log_{10}(l_s/\sqrt{D_0/\Delta\omega})$. Only signals larger than 10^{-6} are displayed.

to plot time in units of the inverse linewidth, i.e., to plot $\Delta\omega t$ and to express the size in units of $\sqrt{D_0/\Delta\omega}$, which is the typical length a spin diffuses in a time $1/\Delta\omega$.

The asymptotic expressions are applicable when the shortest length scale is much shorter than the other lengths. When the two shortest lengths are comparable, there will be some deviations. This occurs along the two lines running down the surface of Fig. 1. When l_g approaches l_D along the line $(\Delta\omega t)^3 = (l_s/\sqrt{D_0/\Delta\omega})^2$, the full solution will show a less abrupt change of slope. There is also some extra structure near the line when l_s approaches l_g, i.e., when $l_s/\sqrt{D_0/\Delta\omega} = 1$ (*18*). Even with this limitation, Fig. 1 captures the dominant features of the Hahn echo decay in this system. The motional averaging regime appears on the left-hand side of Fig. 1. The smaller the pores, the better diffusion averages the field inhomogeneities and the slower the decay (even though the gradients become larger). As the size l_s is increased, the behavior goes over to the free diffusion regime, which at a later time crosses over into the localization regime. The larger the l_s, the smaller the gradient and the slower the decay. For a given inhomogeneity, $\Delta\omega$, the fastest decay occurs when $l_s \simeq \sqrt{D_0/\Delta\omega}$. This is also the condition that the dephasing length l_g and the structural length l_s coincide: $l_s \simeq l_g$.

CPMG PULSE SEQUENCE

In downhole NMR measurements, the CPMG pulse sequence is used instead of the simple Hahn echo in order to maximize the ratio of signal-to-noise. This sequence consists of an initial $\pi/2$ pulse, followed by a train of π pulses, each separated by a time t_E from the previous π pulse. Echoes form between the π pulses. The analysis presented above was based on the Hahn echo. It must be adapted to the case of the CPMG sequence, where an additional length scale is entering the problem, namely $l_E \equiv \sqrt{D_0 t_E}$. We discuss the asymptotic behavior for the regimes of very large and very small pores. We note that restricted diffusion in the presence of a gradient for intermediate regimes has not been fully analyzed for the CPMG sequence. Tarczon and Halperin (*19*) made an analysis based on the Gaussian phase approximation.

In the free diffusion regime (large pores), l_E is now the shortest length scale and the signal starts to decay according to the well-known expression

$$M(t)/M_0 = \exp\{-\tfrac{1}{12} D_0 \gamma^2 g^2 t_E^2 t\}. \qquad [4]$$

In this expression, t is the time at the kth echo, i.e., $t = kt_E$.

In the motional averaging regime (small pores) when $l_E \gg l_s$, the decay will follow Eq. [2] and show no dependence on t_E. When t_E becomes shorter than l_s^2/D_0, we expect that the behavior goes over to Eq. [4].

We want to focus on the dependence of the signal decay on the echo spacing, t_E. In large pores, when the spins are predominantly in the free diffusion regime, Eq. [4] indicates a strong dependence on t_E. In small pores, we expect that the relaxation rate first increases a bit and then stays constant for values of t_E larger than l_s^2/D_0. In this motional averaging regime, there is no dependence on t_E. The contribution to the decay rate of diffusion cannot be distinguished by its t_E dependence from other contributions, such as surface or bulk relaxation. However, note that for smaller and smaller pore sizes, Fig. 1 shows that the diffusion contribution to the signal decay decreases rapidly and becomes unimportant.

EFFECTIVE GRADIENTS IN SEDIMENTARY ROCKS

How do we generalize from the simple model discussed above to sedimentary rocks? In rocks, the field variations caused by the susceptibility differences are clearly more complicated than can be described by a constant gradient. However, a given spin does not diffuse very far during the NMR measurement. The question arises, whether the local field variation can be adequately modeled by some local effective field gradient. We make a heuristic argument below that this effective field gradient is related to the field variations over the local dephasing length and has an upper limit. The total signal decay is then to first order a superposition of the signal decay of subsets of spins, each of which experiences a local effective gradient and can be in the free diffusion regime or the motional averaging regime, depending on the pore size. This is somewhat similar to the earlier work by Bendel (*20*). He considered the superposition of signals from spins in the local gradient. We will argue that the relevant gradient is an effective gradient that is a specific average of the local gradient.

In sedimentary rocks, spins are not confined to individual pores; they can diffuse from one pore to the next. It is also often impossible to divide the pore space unambiguously into individual pores, because the whole pore space is in general connected. However, even in such a system, it is possible that the motional averaging regime applies, because it was pointed out by Wayne and Cotts (*21*) that diffusion in an isolated pore with a constant gradient is equivalent to unbounded diffusion with a periodic gradient.

The following key question must be answered: What is the proper scale for subdividing the spins into subsets? For NMR diffusion measurements, it is natural to label spins according to their local Larmor frequency. Diffusion in the field inhomogeneity leads to an uncertainty in this value. The time-dependent Larmor frequency of a spin can be measured only to an accuracy $\delta\omega$ if the spin stays a time long compared with $1/\delta\omega$ in the appropriate field. Therefore, the size of the subset, l_c, should be chosen such that all spins within a subset have the same Larmor frequency within the uncertainty imposed by diffusion. This implies that across the size of the subset, l_c, the uncertainty in Larmor frequency, $\Delta\omega = |\omega(x) - \omega(x + l_c)|$, becomes equal to D_0/l_c^2. We describe the field inhomogeneity across the size of the subset by the local effective gradient $g_{\text{eff}}(x)$: $\Delta\omega(x) \approx \gamma g_{\text{eff}}(x)x$. The size of the subset l_c is then identical to l_g introduced above, using the effective gradient g_{eff}:

$$l_c = l_g(x) = \left(\frac{D_0}{\gamma g_{\text{eff}}(x)}\right)^{1/3}. \qquad [5]$$

The field inhomogeneities must be averaged over the length l_g to obtain the effective gradient g_{eff}, with the additional restriction that the two quantities l_g and g_{eff} are related to each other by Eq. [5]. If the real field inhomogeneity is described by a uniform gradient g, the effective gradient is identical to g: $g = g_{\text{eff}}$. Le Doussal and Sen (*22*) studied the case of a parabolic field profile: $B = B_0 + g_2(z - z_0)^2$. At the field extremum, the size of the subset calculated by the method outlined above becomes $l_g(z_0) = (D_0/\gamma g_2)^{1/4}$, which is in agreement with their exact calculation.

The length scale $l_g(x)$ is typically in the range of a few to tens of micrometers. Structure in the field profile on a length scale shorter than l_g is not important, because it gets averaged out by diffusion.

This allows us to classify the pore space into ''large'' and ''small'' pores or subsets. In the large pores, the pore size is large compared to the local dephasing length $l_g(x)$ and the echo dephasing is essentially governed by the free diffusion regime. In the small pores, the pore size is small compared to $l_g(x)$ and the internal field inhomogeneities are motionally averaged.

In large pores, the dephasing length is by definition smaller than the pore size. Therefore, we can assume essentially free diffusion. We ignore more subtle effects at longer times: The small number of spins close to the surfaces that have experienced restricted diffusion have decayed less and might dominate the signal. On the other hand, they are also more likely to decay due to surface relaxation. This second-order effect depends on the details of pore size, shape, and surface relaxivity and will not be further discussed.

The spins in the large pores will experience some local, effective gradient $g_{\text{eff}}(x)$. This effective gradient is obtained by averaging the field inhomogeneities self-consistently over the length $l_g(x)$, as discussed above. The echo attenuation due to diffusion in the susceptibility-induced field inhomogeneities is then determined by the distribution of effective gradients, $f(g_{\text{eff}})$, for the large pores. To first order, we obtain for large pores

$$M(t)/M_0 \approx \int_0^{g_{\max}} dg_{\text{eff}}\, f(g_{\text{eff}}) \times \exp\left\{-\frac{1}{12} D_0\gamma^2 g_{\text{eff}}^2 t_E^2 t\right\}. \qquad [6]$$

We have indicated in [6] that there is an upper limit of g_{eff}. The reason is that the total variation in the local field is effectively bounded by $\Delta\chi B_0$, as was shown by Brown and Fantazzini (*9*). The effective gradient g_{eff} is associated with a length l_g given by Eq. [5]. This implies directly that $g_{\text{eff}} l_g \leq \Delta\chi B_0$. Using the expression Eq. [5] for l_g and solving for g_{eff} leads to the approximate upper limit $g_{\max}$:

$$g_{\max} \approx \left(\frac{\gamma}{D_0}\right)^{1/2} (\Delta\chi B_0)^{3/2}. \qquad [7]$$

An effective gradient of $g_{\max}$ defines a scale for structural features of the order of the associated dephasing length, namely,

$$l^* = \frac{\Delta\chi B_0}{g_{\max}} = \left(\frac{D_0}{\gamma\Delta\chi B_0}\right)^{1/2}. \qquad [8]$$

The size l^* is the relevant size for distinguishing small and large pores.

There is another argument that there must be a maximal effective gradient that scales like the expression given in Eq. [7]. For $g_{\max}$, the signal decay given by Eq. [4] is proportional to $(\gamma\Delta B_0)^3 t_E^2$. The maximal value for t_E for which this expression applies should be of order $(l^*)^2/D_0 = (\gamma\Delta B_0)^{-1}$. For this value of echo spacing, the maximal decay rate becomes proportional to $\gamma\Delta B_0$. This is the static linewidth and the decay rate of the free induction decay. It is clear that the amplitudes of the spin echoes cannot decay any faster than the free induction decay.

MAXIMAL EFFECTIVE GRADIENTS IN SEDIMENTARY ROCKS

All the gradients in the pore space scale like the linewidth, $\Delta\chi B_0$, but the largest possible effective gradients, given by Eq. [7], scale with the 3/2 power of $\Delta\chi B_0$. The reason is that the largest effective gradient comes from the smallest large pores as defined above. They have an approximate size l^*, which leads to a gradient of $g_{max} \simeq \Delta\chi B_0/l^*$. The critical length l^* depends on the inverse square root of field strength, as given in Eq. [8], thus leading to the 3/2 power dependence for g_{max}.

At small enough field strength, the gradient in a small pore is averaged out by diffusion, resulting in an effective gradient much smaller than the local gradient of the magnetic field. As the field strength is increased, the variation in magnetic field becomes large enough that diffusion cannot efficiently average it out anymore. In this case, the effective gradient and the local field gradient will approach each other.

In what circumstances are these susceptibility-induced effective gradients in rocks affecting the results of NMR well logging? In NMR well logging, the applied magnetic field in the sensitive region is relatively low (a few hundred gauss), but it is unavoidably nonuniform. The static tool gradients in commercial logging tools (*11, 12*) are in the range of a few tens of gauss per centimeter. If it is assumed that the field inhomogeneities are dominated by these known tool gradients, then it is possible to estimate the diffusion coefficient of the unknown fluid from the t_E dependence of the signal decay, assuming unrestricted diffusion (*13*). This procedure of fluid characterization is robust only if the typical size of the effective gradient due to the susceptibility mismatch is negligible compared to the applied tool gradients. Dephasing in strong internal gradients would lead to an incorrect estimate of the diffusion coefficient of the fluid.

Equation [7] allows us to estimate the upper limit of effective gradients based on susceptibility measurements only. In Fig. 2 a histogram of all the susceptibilities of sedimentary rocks measured in our rock lab between 1989 and 1994 is shown. The bottom axes show the absolute value of the susceptibility difference between the rock grains and water ($\chi[H_2O] = -9.05 \times 10^{-6}$), whereas the top axes indicate the maximal effective gradients g_{max} deduced from Eq. [7], using values of $D_0 = 2.3 \times 10^{-5}$ cm^2/s and $B_0 = 550$ G. This corresponds to a Larmor frequency of 2.3 MHz, which is typical of current commercial logging tools.

The distribution of susceptibility differences is several orders of magnitude wide, reflecting the wide variation in paramagnetic impurities, mainly iron and manganese, in sedimentary rocks. However, there is a clear trend of larger susceptibility differences in sandstones compared to those of carbonates, on average by about an order of magnitude. The majority of carbonate rocks is diamagnetic, whereas almost all sandstones are paramagnetic. Both pure calcium carbonate and quartz are diamagnetic, but sandstones tend to have a larger amount of paramagnetic impurities than carbonates.

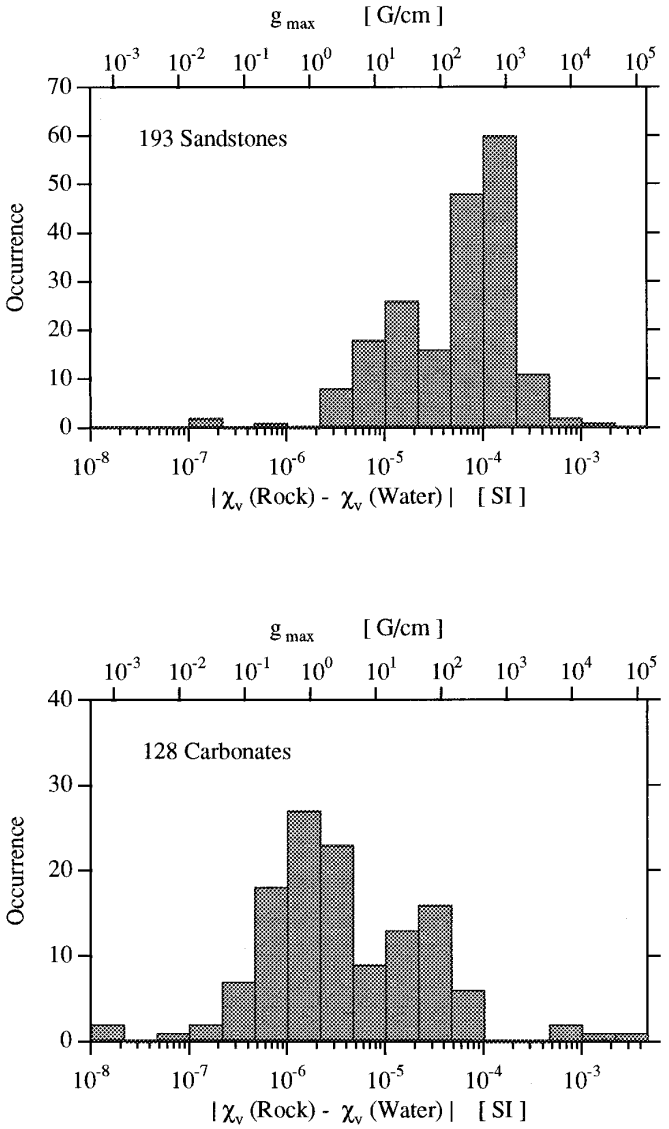

FIG. 2. Histogram of the values of susceptibilities measured at SDR. Results for sandstones are shown at the top, and results for carbonates are shown at the bottom. The top axes indicate the corresponding values of g_{max} calculated from Eq. [7] for the diffusion coefficient of water at room temperature and a static field $B_0 = 550$ G.

The maximal possible effective gradients, g_{max}, indicated on the top axes are obtained from Eq. [7]. This relationship is essentially a dimensional analysis and is clearly only a rough estimate. Given a susceptibility difference, we expect the largest effective gradients for pores with structure on a length scale l^*, Eq. [8]. If the pore space has structure on that length scale, the expected gradient in those pores is then of order g_{max}. Larger internal gradients might occur if the susceptibility of the rock grains is heterogeneous.

TABLE 1
Measured Susceptibility Differences and Calculated Values of Maximal Effective Gradient and Critical Length

Sample	$\Delta\chi$ [SI]	g_{max} at 2 MHz	l^*
C9	278×10^{-6}	1800 G/cm	0.8 μm
Berea 100	98.9×10^{-6}	375 G/cm	1.3 μm
Berea 400/500	33.8×10^{-6}	75 G/cm	2.3 μm
A7	13.6×10^{-6}	19 G/cm	3.6 μm
Indiana limestone	2.99×10^{-6}	2.0 G/cm	7.6 μm
Mudstone	1.22×10^{-6}	0.5 G/cm	11.9 μm

Even though Eq. [7] is only a rough estimate, we can conclude that in the majority of carbonates, the value of g_{max} is smaller than typical tool gradients. Therefore, the vast majority of local effective gradients in carbonates are smaller than tool gradients. The situation is different in sandstones. At the peak of the susceptibility distribution for sandstones, we estimate that internal gradients can be as large as 1000 G/cm for a Larmor frequency of only 2.3 MHz. In sandstones, internal gradients can therefore frequently be comparable to or larger than tool gradients.

At downhole temperatures, the estimated values for g_{max} are reduced by a factor of 2.5 because the diffusion coefficient is higher and the susceptibilities are reduced (assuming Curie law behavior). Based on this analysis we expect that the effective gradients in most carbonates are smaller than the tool gradients and can mostly be ignored. However, in many sandstones, the effective gradients can be significantly larger than tool gradients. This clearly complicates the analysis of diffusion measurements with static applied tool gradients in sandstones.

EXPERIMENTAL NMR RESULTS

CPMG measurements were performed on six water-saturated sedimentary rocks with susceptibility differences ranging from about 10^{-6} to over 2×10^{-4}. Table 1 lists the measured values of $\Delta\chi$ and the calculated values of g_{max} (Eq. [7]) and l^* (Eq. [8]). Note that these samples cover the typical susceptibility differences of sedimentary rocks, shown in Fig. 2. The NMR measurements were performed at 2 MHz with a laboratory NMR spectrometer that has a homogeneous external magnetic field and the temperature was 25°C. Eight different echo spacings, t_E, were used, namely 160, 200, and 400 μs and 1, 2, 4, 10, and 20 ms. Data were collected up to a total time of 655 ms; i.e., the number of echoes collected was adjusted to between 4095, for $t_E = 160$ μs, and 33, for $t_E = 20$ ms.

In water-saturated sedimentary rocks, the transverse relaxation rate at low field strength is usually dominated by surface relaxation; relaxation caused by internal gradients only dominates for longer echo spacings t_E. The surface relaxation is typically nonexponential and can be described by a distribution of relaxation times, $h(T_2)$, for T_2 values in the range between about 1 ms and 1 s:

$$M(t, t_E) \approx \int dT_2 \int_0^{g_{max}} dg_{eff}\, f(g_{eff}) \times \exp\left\{-\frac{1}{12} D_0 \gamma^2 g_{eff}^2 t_E^2 t\right\} \times h(T_2) \exp\{-t/T_2\}. \quad [9]$$

Here $f(g_{eff})$ is the distribution of effective gradients and $h(T_2)$ is the distribution of relaxation time T_2. As discussed above, $h(T_2)$ includes surface relaxation and diffusive contributions from the small pores. At the shortest echo spacing $t_E = 160$ μs, the T_2 term dominates the gradient term. If we can make the further assumption that the two terms are not highly correlated, we obtain for the ratio of $M(t, t_E)/M(t, t_E = 160\ \mu s)$ the simple form

$$\frac{M(t, t_E)}{M(t, t_E = 160\ \mu s)} \approx \int_0^{g_{max}} dg_{eff}\, f(g_{eff}) \times \exp\left\{-\frac{1}{12} D_0 \gamma^2 g_{eff}^2 t_E^2 t\right\}. \quad [10]$$

This predicts that the ratio $M(t, t_E)/M(t, t_E = 160\ \mu s)$ is to first order only a function of the combined times $t_E^2 t$. In Fig. 3, this ratio is plotted as a function of $t_E^2 t$ for the six rocks listed in Table 1.

In Fig. 3, we note first of all that for all six rocks, there is a reasonable collapse of the data on a single curve. To first approximation, the ratio is indeed only a function of $t_E^2 t$, as given in Eq. [10]. This is not completely obvious. One might argue that for any given time t, there is a different distribution of effective gradients. At long time, surface relaxation relaxes the spins in the smaller pores and only the spins in the larger pores survive. One would expect that the distribution at long times is dominated by smaller gradients, whereas at shorter times, spins in both small and large pores contribute. A careful analysis of the data for C9 and the Bereas shows that the scatter in Fig. 3 is in fact somewhat correlated with time t; i.e., at a given value of $t_E^2 t$, ratios for large t tend to be somewhat higher than ratios for small t. However, this is a rather weak effect and indicates that surface relaxation and diffusion in internal gradients are sensitive to different features of the pore geometries. Diffusion is sensitive to features of size l^*, whereas surface relaxation is sensitive to the ratio of the surface area to pore volume.

The arrows in Fig. 3 mark the value of $t_E^2 t$ where $\frac{1}{12} D_0 \gamma^2 g_{max}^2 t_E^2 t = 1$. Using the expression in Eq. [7], this is simply given by $t_E^2 t = 12/(\gamma \Delta\chi B_0)^3$. This is the $1/e$ point for the largest possible effective gradient. We expect no

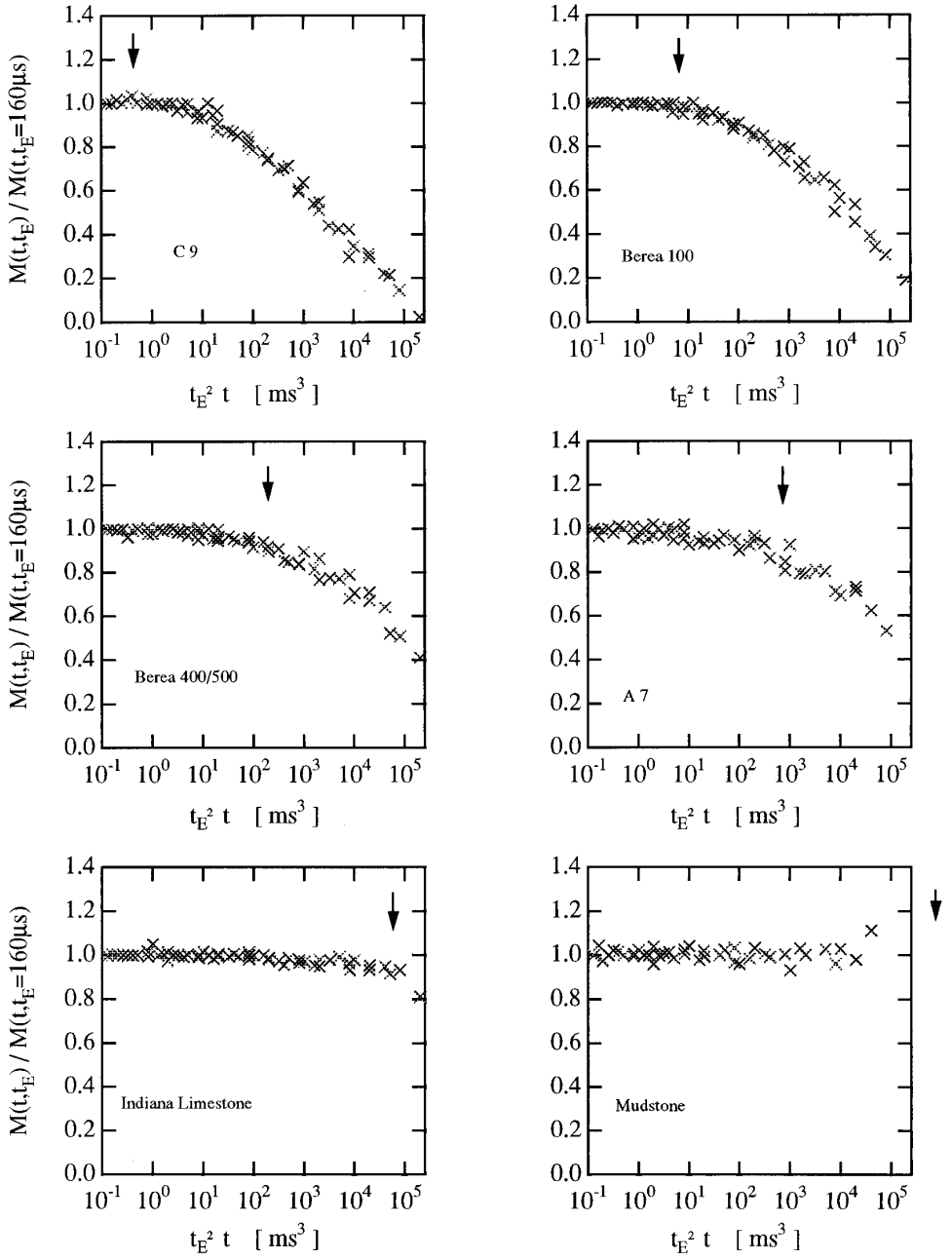

FIG. 3. Ratio of $M(t, t_E)/M(t, t_E = 160\ \mu s)$ versus $t_E^2 t$ for six different rocks. In all cases, there is a good data collapse for all the different values of t and t_E, spanning $t_E^2 t$ over six orders of magnitude. The arrow indicates the $1/e$ point for the largest effective gradient as calculated from the susceptibility difference between the rock and water.

significant deviation of the ratio $M(t, t_E)/M(t, t_E = 160\ \mu s)$ from 1 for values of $t_E^2 t$ smaller than indicated by the arrows. This simple estimate is in good agreement with the observations. This is especially noteworthy because the prediction has no adjustable parameters and depends only on susceptibility and Larmor frequency. Note that it covers several order of magnitudes: for a given value of t_E, the diffusion-induced decay rate varies by six orders of magnitude in these rocks.

In order for the signal to show decay at the maximal gradient, there must be structure on the length scale l^* given in Table 1. The curve for C9 in Fig. 3 appears to decrease only at values of $t_E^2 t$ that are about a decade larger than shown by the arrow. In this rock, the pore space might not have a lot of structure on the length scale of 0.8 μm. Alternatively, it is possible that the decay for $t_E = 160\ \mu s$ is already affected by diffusion in the internal gradients.

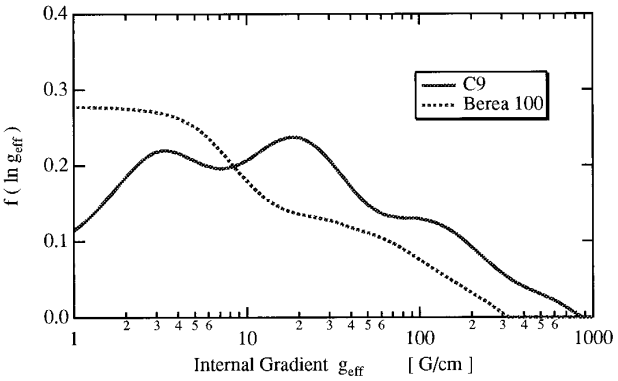

FIG. 4. Estimate of the distribution of internal gradients in the two rocks with the largest susceptibility difference.

Using Eq. [10], we can estimate the distribution of effective internal gradients, $f(g_{\text{eff}})$, from the data shown in Fig. 3. We use a fitting routine based on single value decomposition. The routine was implemented by Sezginer and is described in (*23*) where it is applied to relaxation data. The results for the two rocks with the largest susceptibility differences, C9 and Berea 100, are shown in Fig. 4.

These distributions are several decades wide and both have a significant fraction of gradients above 100 G/cm, as expected.

CONCLUSIONS

In this report, we have analyzed the signal decay caused by diffusion in internal gradients. We have shown that the pores can be classified into large or small pores, by comparing the pore size to $\sqrt{D_0/\gamma\Delta\chi B_0}$. Only the contributions from the large pores show a significant increase of the decay rate with echo spacing t_{E}. This decay can be described to first order by a distribution of effective gradients. It is argued that there is a maximum value for the effective gradient, $g_{\max}$, that depends only on diffusion coefficient, Larmor frequency, and susceptibility difference.

This analysis was then applied to the study of water-saturated sedimentary rocks, relevant in NMR well logging. From a compilation of susceptibility measurements, we conclude that the effective gradients in carbonates are typically smaller than tool gradients, whereas in many sandstones, internal gradients can be comparable to tool gradients. This complicates the analysis of diffusion measurements in sandstones. CPMG measurements with different echo spacings on six rocks confirm these theoretical predictions.

In biological systems, the susceptibility differences encountered are usually smaller than those in sedimentary rocks, but the measurements are typically performed at Larmor frequencies much higher than 2 MHz. This analysis should therefore also be relevant for these systems.

ACKNOWLEDGMENTS

I had helpful discussions with P. Sen, R. Kleinberg, K. Helmer, and B. Halperin. The CPMG measurements were performed by D. Rossini, and P. Dryden and W. Smith assisted me with the susceptibility data.

REFERENCES

1. K. K. Kwong, J. W. Belliveau, D. A. Chesler, I. E. Goldberg, R. M. Weisskoff, B. P. Poncelet, D. N. Kennedy, B. E. Hoppel, M. S., Cohen, R. Turner, H.-M. Cheng, T. J. Brady, and B. R. Rosen, *Proc. Natl. Acad. Sci. USA* **89,** 5675 (1992).
2. S. Ogawa, D. W. Tank, R. Menon, J. M. Ellermann, S.-G. Kim, H. Merkle, and K. Ugurbil, *Proc. Natl. Acad. Sci. USA* **89,** 5952 (1992).
3. R. N. Muller, P. Gillis, F. Moiny, and A. Roch, Transverse relaxivity of particulate MRI contrast media: From theories to experiments, *Magn. Reson. Med.* **22,** 178 (1991).
4. P. Hardy and R. M. Henkelman, On the transverse relaxation rate enhancement induced by diffusion of spins through inhomogeneous fields, *Magn. Reson. Med.* **17,** 348 (1991).
5. R. M. Weisskoff, C. S. Zuo, J. L. Boxerman, and B. R. Rosen, Microscopic susceptibility variation and transverse relaxation: Theory and experiment, *Magn. Reson. Med.* **31,** 601 (1994).
6. R. L. Kleinberg, ''Encyclopedia of Nuclear Magnetic Resonance,'' Vol. 8, pp. 4960–4969, Wiley, Chichester (1996).
7. R. L. Kleinberg and M. A. Horsfield, Transverse relaxation processes in porous sedimentary rock, *J. Magn. Reson.* **88,** 9 (1990).
8. R. L. Kleinberg, Pore size distributions, pore coupling, and transverse relaxation spectra of porous rocks, *Magn. Reson. Imaging* **12,** 271 (1994).
9. R. J. S. Brown and P. Fantazzini, Conditions for initial quasilinear T_2^{-1} versus τ for Carr–Purcell–Meiboom–Gill NMR with diffusion and susceptibility differences in porous media and tissues, *Phys. Rev. B* **47,** 14823 (1993).
10. G. C. Borgia, R. J. S. Brown, and P. Fantazzini, Scaling of spin-echo amplitudes with frequency, diffusion coefficient, pore size, and susceptibility difference for the NMR of fluids in porous media and biological tissues. *Phys. Rev. E* **51,** 2104 (1995).
11. Z. Taicher, G. Coates, Y. Gitartz, and L. Berman, A comprehensive approach to studies of porous media (rocks) using a laboratory spectrometer and logging tool with similar operating characteristics, *Magn. Reson. Imaging* **12,** 285 (1994).
12. R. L. Kleinberg, A. Sezginer, and D. D. Griffin, Novel NMR apparatus for investigating an external sample, *J. Magn. Reson.* **97,** 466 (1992).
13. R. Akkurt, H. J. Vinegar, P. N. Tutunjian, and A. J. Guillory, NMR logging of natural gas reservoirs, *in* ''Trans. SPWLA 36th Annual Logging Symposium, Paris, 1995,'' Paper N.
14. S. D. Stoller, W. Happer, and F. J. Dyson, Transverse spin relaxation in inhomogeneous magnetic fields, *Phys. Rev. A* **44,** 7459 (1991).
15. T. M. de Swiet and P. N. Sen, Decay of nuclear magnetization by bounded diffusion in a constant field gradient, *J. Chem. Phys.* **100,** 5597 (1994).
16. M. D. Hürlimann, K. G. Helmer, T. M. de Swiet, P. N. Sen, and C. H. Sotak, Spin echoes in a constant gradient and in the presence of simple restriction, *J. Magn. Reson. A* **113,** 260 (1995).
17. C. H. Neuman, Spin echo of spins diffusing in a bounded medium, *J. Chem. Phys.* **60,** 4508 (1974).

18. M. H. Blees, The effect of finite duration of gradient pulses on the pulsed-field-gradient NMR method for studying restricted diffusion, *J. Magn. Reson. A* **109,** 203 (1994).

19. J. C. Tarczon and W. P. Halperin, Interpretation of NMR diffusion measurements in uniform- and nonuniform-field profiles. *Phys. Rev. B* **32,** 2798 (1985).

20. P. Bendel, Spin-echo attenuation by diffusion in nonuniform field gradients, *J. Magn. Reson.* **86,** 509 (1990).

21. R. C. Wayne and R. M. Cotts, Nuclear-magnetic-resonance study of self-diffusion in a bounded medium, *Phys. Rev.* **151,** 264 (1966).

22. P. Le Doussal and P. N. Sen, Decay of nuclear magnetization by diffusion in a parabolic magnetic field: An exactly solvable model, *Phys. Rev. B* **46,** 3465 (1992).

23. E. J. Fordham, A. Sezginer, and L. D. Hall, Imaging multiexponential relaxation in the $(y, \log_e T_1)$ plane, with application to clay filtration in rock cores, *J. Magn. Reson. A* **113,** 139 (1995).